Rational design of a ligand-controlled protein conformational switch

Onur Dagliyan[a,b,c,1], David Shirvanyants[a,1], Andrei V. Karginov[c], Feng Ding[a], Lanette Fee[a], Srinivas N. Chandrasekaran[a,b], Christina M. Freisinger[d], Gromoslaw A. Smolen[d], Anna Huttenlocher[d], Klaus M. Hahn[c,2], and Nikolay V. Dokholyan[a,b,2]

[a]Department of Biochemistry and Biophysics, [b]Program in Molecular and Cellular Biophysics, and [c]Department of Pharmacology, School of Medicine, University of North Carolina, Chapel Hill, NC 27599; and [d]Department of Medical Microbiology, University of Wisconsin, Madison, WI 53706

Edited by Harold A. Scheraga, Cornell University, Ithaca, NY, and approved March 18, 2013 (received for review October 19, 2012)

Design of a regulatable multistate protein is a challenge for protein engineering. Here we design a protein with a unique topology, called uniRapR, whose conformation is controlled by the binding of a small molecule. We confirm switching and control ability of uniRapR *in silico*, in vitro, and in vivo. As a proof of concept, uniRapR is used as an artificial regulatory domain to control activity of kinases. By activating Src kinase using uniRapR in single cells and whole organism, we observe two unique phenotypes consistent with its role in metastasis. Activation of Src kinase leads to rapid induction of protrusion with polarized spreading in HeLa cells, and morphological changes with loss of cell–cell contacts in the epidermal tissue of zebrafish. The rational creation of uniRapR exemplifies the strength of computational protein design, and offers a powerful means for targeted activation of many pathways to study signaling in living organisms.

spatiotemporal control | cell motility | endothelial-mesenchymal transition

The past two decades have seen a revolution in computational protein design, with remarkable milestones including design of a helical protein from first principles (1), redesign of zinc finger proteins (2), and de novo design of an α/β protein (3). These studies highlighted, as a proof of principle, our ability to rationally control the structure of proteins by using basic physical principles and phenomenology. These approaches are based on finding an optimal sequence for a given single structure or ensemble of related states, and do not provide a strategy to construct a protein capable of large on-demand conformational transitions (4, 5). A number of multistate protein design algorithms (4, 6) have been proposed; however, designing an experimentally confirmed, regulatable multistate protein, or a conformational switch (5), still remains as a challenging task because of the necessity of engineering and controlling multiple protein states (4, 7, 8).

Such a conformational switch protein has great advantages in cell signaling, because it can be used as a universal regulatory domain (9) for precise, specific, and temporal control over rapidly activated signaling proteins (5, 10–15). Traditional genetically encoded methods for temporal protein control at the protein level have several drawbacks (5, 13). Recently developed protein switches, including derivatives of the light, oxygen, or voltage (LOV) domain (16, 17), can provide direct control at the protein level with light, but cannot be readily used in non-transparent animals. Our previous rapamycin regulated (RapR) kinase method (14) can potentially overcome this problem, but it requires expression and control of two proteins. The variable stoichiometry of these proteins renders the response more heterogeneous and essentially impractical in animals. Therefore, a single-chain, insertable, and transferable regulatory domain would be very valuable.

Here we design a ligand-controlled conformational switch, uniRapR, a potentially broadly applicable, single-chain regulatory domain. We first confirm its switching properties and control ability with molecular dynamics and in vitro enzymatic assays. Further, by temporally activating Src kinase with uniRapR in living single cells and zebrafish, we reveal two phenotypes related to the role of this kinase in metastasis.

Results

Design of uniRapR with Desired Stability and Conformational Dynamics. Design of ligand binding proteins is still an unsolved problem in protein design (18); therefore, to design a ligand-controlled protein, we first use the binding pocket of one of the highest-affinity (19) protein–ligand complexes, 12-kDa FK506-binding protein (FKBP12) and FKBP12-rapamycin binding protein (FRB) in complex with rapamycin (20). We rationally rewired this complex to build a single-chain protein featuring a unique topology (21) (Fig. 1*A* and Fig. S1). To construct the subdomain-A of uniRapR, we used elements of insertable FKBP12 (iFKBP), a modified FKBP; we previously demonstrated that its insertion does not destroy the structure of a host protein (14). Subdomain-B of uniRapR contains the rapamycin-binding surface of FRB, and we stabilized this surface with two helices grafted from FRB. Thus, we expect the resulting design has all the desired properties of a universal regulatory domain featuring modularity, transferability, and robust switching ability.

To test conformational switching features of uniRapR, we constructed a structural model of uniRapR based on complex structure of FKBP-FRB–rapamycin and performed replica exchange and equilibrium discrete molecular dynamics (DMD) simulations (22, 23) (Fig. 1*B* and *Materials and Methods*). Previous studies that used insertable FKBP showed that the transition between a folded and unfolded state could be used to control kinase activity when the FKBP was inserted at a conserved site in kinases. Therefore, desired switching properties of uniRapR were achieved by manipulating the subdomain motions and changing the relative stability between the folded and unfolded states. We estimated the stability of uniRapR states by characterizing its folding thermodynamics. We calculated its specific heat and the root-mean-square deviations (rmsds) from the native structure of iFKBP as a function of temperature. A peak in the specific heat curve corresponds to the folding transition, indicated by significant increase of rmsd (Fig. 1 *C* and *D*). We observed the stabilization of uniRapR upon rapamycin binding as a shift of the peak of the specific heat curve to a higher temperature. UniRapR can achieve regulatory function when inserted into a host kinase because its thermal stability and

Author contributions: O.D., D.S., K.M.H., and N.V.D. designed research; O.D., D.S., A.V.K., L.F., C.M.F., and G.A.S. performed research; S.N.C. contributed new reagents/analytic tools; O.D., D.S., A.V.K., F.D., L.F., A.H., K.M.H., and N.V.D. analyzed data; and O.D., K.M.H., and N.V.D. wrote the paper.

The authors declare no conflict of interest.

This article is a PNAS Direct Submission.

[1]O.D. and D.S. contributed equally to this work.

[2]To whom correspondence may be addressed. E-mail: dokh@unc.edu or khahn@med.unc.edu.

This article contains supporting information online at www.pnas.org/lookup/suppl/doi:10.1073/pnas.1218319110/-/DCSupplemental.

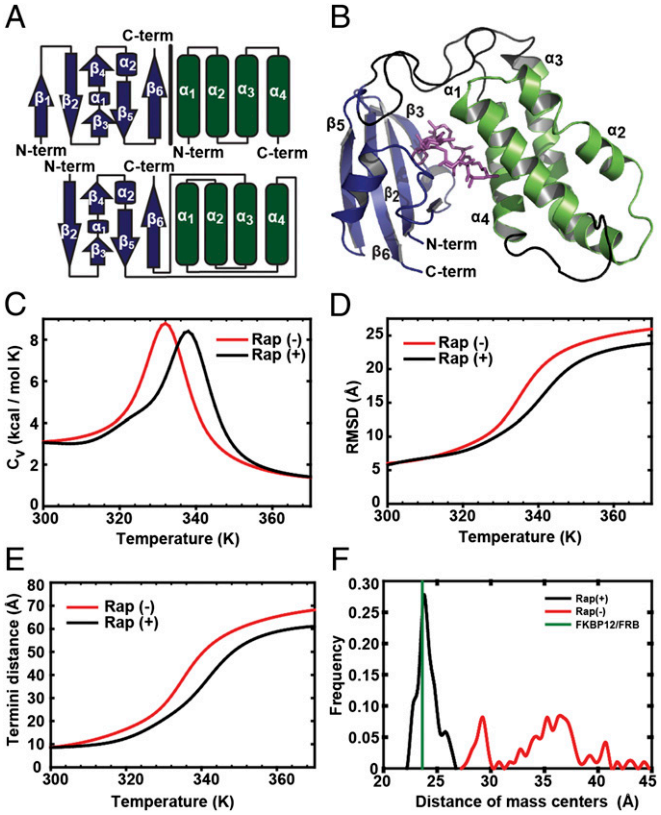

Fig. 1. Design and thermodynamics of uniRapR domain. (*A*) The FKBP12 (blue)/FRB (green) complex was used to build the switch module (Fig. S1). While keeping the sequence from β2 to β5 of iFKBP, we linked β5 of subdomain-A to the carboxyl-terminal α-helix (α4) of subdomain-B by using an optimized GS linker to permit a hinge-like motion. Because the N terminus of α1 is relatively close to the C terminus of α4, we linked these two helices using a PPGPGSG linker. Sequences of helices α2 and α3 were kept as in WT FRB, and α3 was linked to the C-terminal β-strand (β6) of subdomain A, as the N terminus of β6 of FKBP is in the vicinity of the ternary complex interface. (*B*) A model of the holo-uniRapR (blue, subdomain-A; green, subdomain-B) protein was built based on the crystal structure of the FKBP12/FRB complex (Protein Data Bank ID code 1FAP) by using DMD. (*C*) Heat capacities of apo (red) and holo (black) forms of uniRapR were calculated by using WHAM (38). (*D*) rmsd values of apo (red) and holo (black) forms of subdomain-A were calculated for different temperatures by using WHAM. (*E*) Distance between C_α atoms of amino and carboxyl termini as a function of temperature for apo (red) and holo (black) forms of uniRapR. (*F*) Relative positions of uniRapR subdomains compared with the FKBP12/FRB proteins in complex. Distance between centers of masses of uniRapR subdomains A and B was calculated by using multiple molecular dynamics trajectories. In the presence of rapamycin (black), distance of centers of masses of uniRapR subdomains is ~24 Å, close to that of FKBP12 and FRB complex (green). In the absence of rapamycin (red), uniRapR subdomains move randomly, and they are not in contact.

a change in its equilibrium amino- (N-) and carboxy- (C-) termini distance are dependent on rapamycin binding. Indeed, we observed reduced distance between C_α atoms of N- and C-termini upon binding of rapamycin (Fig. 1*E*). Equilibrium simulations confirmed that subdomain-A only interacts with subdomain-B in the presence of rapamycin (Fig. 1*F* and Movies S1 and S2). These observations suggest that the conformation of uniRapR depends on the presence of rapamycin, whereby binding of rapamycin to the pocket formed by the two subdomains stabilizes uniRapR.

Change in ATP Binding Site Dynamics Confer Allosteric Control in Src Kinase. We hypothesize that uniRapR renders a protein switchable when inserted into a site that is allosterically coupled to its active site. Allosteric sites can be identified by using information from experimental mutation studies in the literature or by using various computational methods (24–26). We inserted uniRapR into the Src kinase at a site known (14) to be allosterically coupled to the ATP binding site (Fig. 2). In equilibrium DMD simulations, we observed that uniRapR inserted into Src at residue 288 with optimized double-gly-pro-gly (GPG) linkers destabilized the ATP binding site through long-range interactions, suggesting inactivation of the kinase in the absence of rapamycin. Rapamycin binding to uniRapR reduced fluctuations in the G-loop (residues 276–279), which is part of the ATP binding site. The reduced fluctuations in the presence of rapamycin restored the G-loop dynamics of Src-uniRapR to a level identical to that of WT Src (Fig. 2*B*), implying activation of the kinase in the presence of rapamycin. Computational analysis thus suggests that Src kinase activity can be regulated by inserting uniRapR at a position that is allosterically coupled to the ATP binding site.

UniRapR Allows Specific and Robust Control over Various Kinases in Vitro. We tested uniRapR functionality in vitro by using Src kinase expressed in HEK293T cells. By using paxillin and poly-Glu-Tyr (E4Y) as the Src substrates, we observed that constitutively active (YF) Src kinase (27) modified with uniRapR [uniRapR Src (YF)] demonstrated greatly enhanced activity in the presence of rapamycin, confirming that uniRapR functions as a specific on/off switch (Fig. 2*C* and Figs. S2–S7). A catalytically dead Src mutant (D388R) (14) with inserted uniRapR was inactive regardless of the presence of rapamycin, indicating that rapamycin-induced phosphorylation of paxillin or E4Y is caused by only Src-uniRapR catalytic activity (Fig. 2*C* and Fig. S7). Additionally, when we constrained the hinge motion of the uniRapR domain by substituting the optimized flexible linker (Fig. S2) between subdomains with a rigid poly-proline linker (uniRapR-L1P), catalytic activity in the presence of rapamycin was abolished (Fig. 2*D*). Based on our model and on the crystal structure of the FKBP12/FRB complex showing that Y271 [Y82 in the complex entered with Protein Data Bank ID code 1FAP] is in contact with rapamycin, we expected Y271A substitution to abolish rapamycin binding. We observed dramatically reduced activity of uniRapR Src (Y271A), further indicating that uniRapR Src switching activity is directly dependent on rapamycin binding to uniRapR Src (Fig. 2 *D* and *E*). Significantly, we observed that uniRapR Src has much higher switchable kinase activity than did our previous dimerization-based control of kinase activity (i.e., RapR), in which kinase activity was regulated by using coexpressed WT FRB and iFKBP (14) (Fig. 2*D*). These results indicate that insertion of the uniRapR switch enables us to robustly and specifically control Src kinase activity.

To assess the transferability of the uniRapR switch, we inserted uniRapR into analogous sites of focal adhesion kinase (FAK) and mitogen activated kinase p38. Insertion of uniRapR into a constitutively active mutant (28) of FAK (YM) inhibited the activity of FAK (YM) for its substrate paxillin; addition of rapamycin rescued FAK activity (Fig. 3*A*). Addition of rapamycin did not rescue kinase-dead FAK (YM/KD) activity, suggesting that rapamycin-induced phosphorylation of paxillin is only due to FAK-uniRapR activity. A design with a different circularly permuted version of uniRapR (Fig. S8*A*) did not allow control of FAK activity (Fig. S8*B*). Insertion of uniRapR into p38 kinase with the same GPG linker abolished its activity, which could be restored by the addition of rapamycin. Activity of WT p38 was unchanged in the presence of rapamycin (Fig. 3*B*). Insertion of uniRapR into p38 with an optimized linker described in our previous study (14) resulted in a higher activity in the presence of rapamycin. Indeed, we observed activity similar to WT in the presence of rapamycin (Fig. 3*B*), indicating that optimal regulation of the host protein can be achieved by varying the connection linker. All these data suggest

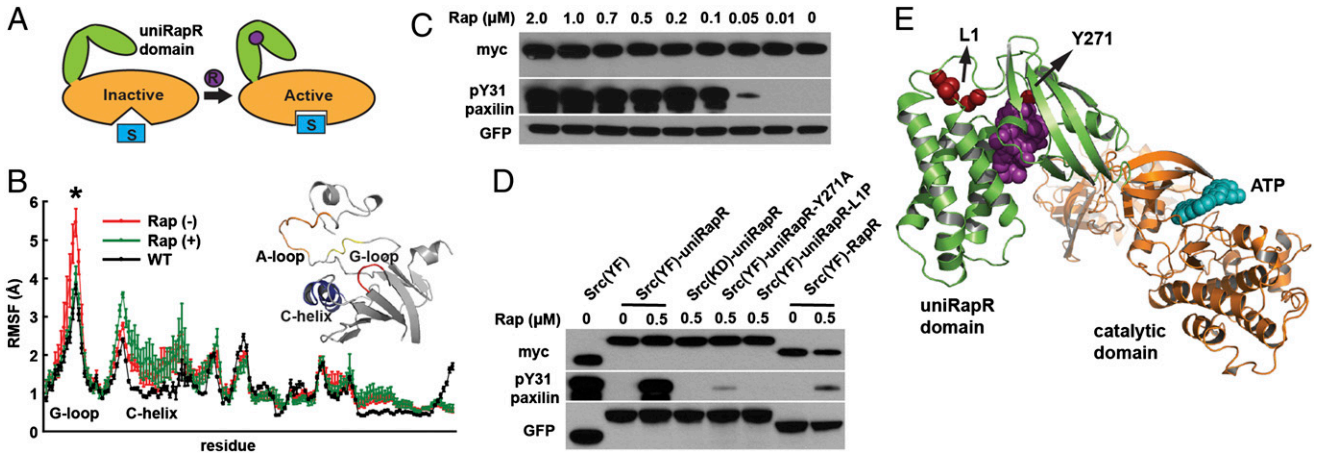

Fig. 2. Control of Src kinase activity with uniRapR domain. (*A*) Schematic representation of activity control with the uniRapR domain. (*B*) Root mean square fluctuations of the ATP binding site (gray structure) based on multiple equilibrium DMD simulations for WT Src (black), apo (red), and holo (green) uniRapR-inserted Src ($P < 0.01$). (*C*) HEK293T cells expressing the Src-uniRapR-cerulean-myc construct were treated with different concentrations of rapamycin (0–2 μM), and lysates were assayed for expression of the construct with Western blotting by using anti-GFP. The construct was pulled down with anti-myc and mixed with the paxillin substrate in the presence of ATP for 10 min. Reaction suspensions were blotted and probed with anti-myc and anti–pY31-paxillin to confirm binding and phosphorylation of the substrate, respectively. (*D*) As controls, constitutively active Src (YF) without the uniRapR domain, kinase dead (YF/KD), Y271A and L1polyP Src mutants with the uniRapR domain, and our previous dimerization-based switch were tested. (*E*) Y271A and L1polyP substitutions shown on the Src-uniRapR model.

that uniRapR can be inserted as a transferable regulatory domain in a wide variety of kinases.

Specific Activation of Src Kinase Leads to Polarized Spreading in Single Cells. Signaling cascades containing Src kinase play important roles in cell growth, proliferation, migration, and tumor invasiveness (27). However, the specific roles of Src catalytic activity, especially in cell migration, are unclear because of the limitations of existing chemical and genetic methods, including limited temporal control of activation or inactivation. For example, overexpression of constitutively active Src prevents the observation of events immediately following Src activation, as the cell compensates for Src expression, probably with other Src kinase family members, during gradual increase in expression level. Likewise, blocking Src expression with RNA interference is also a slow process. We overcome these limitations by using uniRapR Src (YF), which can reach maximal stimulation in less than 3 min.

To observe the effect of Src activation on cell motility, we expressed uniRapR Src (YF) in HeLa cells. In the absence of rapamycin, we observed only peripheral ruffles near the cell edge, a phenotype also seen in untransfected cells. After rapamycin addition, we observed a statistically significant increase in cell area for all cells examined, relative to those expressing catalytically dead Src (YF/KD)-uniRapR (area increase of 30 ± 5%, $n = 8$ cells; Fig. 3 *C* and *D* and Movies S3 and S4). Control cells showed no statistically significant change (area change of 8 ± 6%, $n = 8$ cells). In a control study, rapamycin alone did not have any effect on the phenotype of untransfected cells. Polarized spreading of HeLa cells following Src activation supports a role for Src in cell invasiveness.

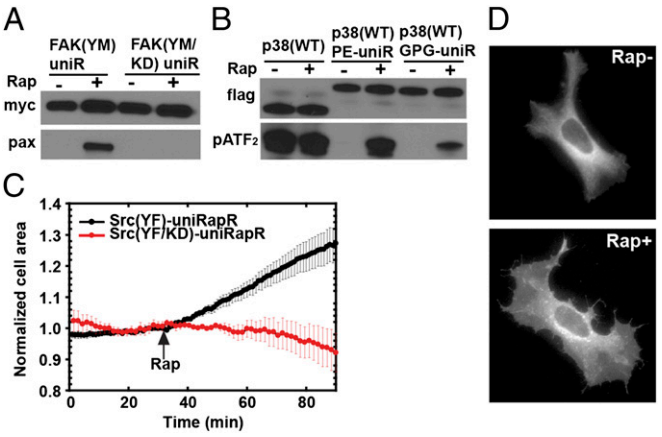

Fig. 3. Testing uniRapR in different kinases and effects of Src activation in HeLa cells. Immunoprecipitation, in vitro FAK (*A*), and p38 (*B*) assays were performed similarly as for Src kinase. (*C*) Change in cell area of HeLa cells expressing Src (YF)-uniRapR (n = 8/8 cells) or Src (YF/KD)-uniRapR (n = 8/8 cells). (*D*) HeLa cells expressing Src-uniRapR (YF)-cerulean demonstrate spreading after the addition of rapamycin.

Specific Activation of Src Kinase Causes Loss of Cell–Cell Contacts in Zebrafish Epidermis. Although we observe a profound impact of Src activation in cultured cells, it is crucial to determine whether uniRapR Src (YF) enables Src activation to be studied in the context of a multicellular organism. To study the role of Src activation during development, we expressed uniRapR Src (YF) in zebrafish embryos (Fig. 4*A*). Epidermal cells expressing uniRapR Src (YF) demonstrated WT polygonal shape and formed tight connections with no gapping in the absence of rapamycin (Fig. 4*B*). When we activated uniRapR Src (YF) by adding rapamycin, the epidermal cells had extended protrusions and underwent significant morphological changes in 12 to 16 h. These morphological changes caused the loss of cell–cell contacts as cells became more rounded (Fig. 4*C*). In control experiments, we did not observe morphological changes when cells expressing uniRapR Src were treated only with vehicle (Fig. 4 *D* and *E*), or when we expressed the catalytically dead uniRapR Src (YF/KD) construct in zebrafish embryos in the presence of rapamycin (Fig. 4 *F* and *G*), demonstrating that the observed effects are caused specifically by uniRapR Src activation by rapamycin. This dramatic phenotype of altered cell morphology upon Src activation demonstrates the applicability of uniRapR in studying signaling pathways in whole organisms.

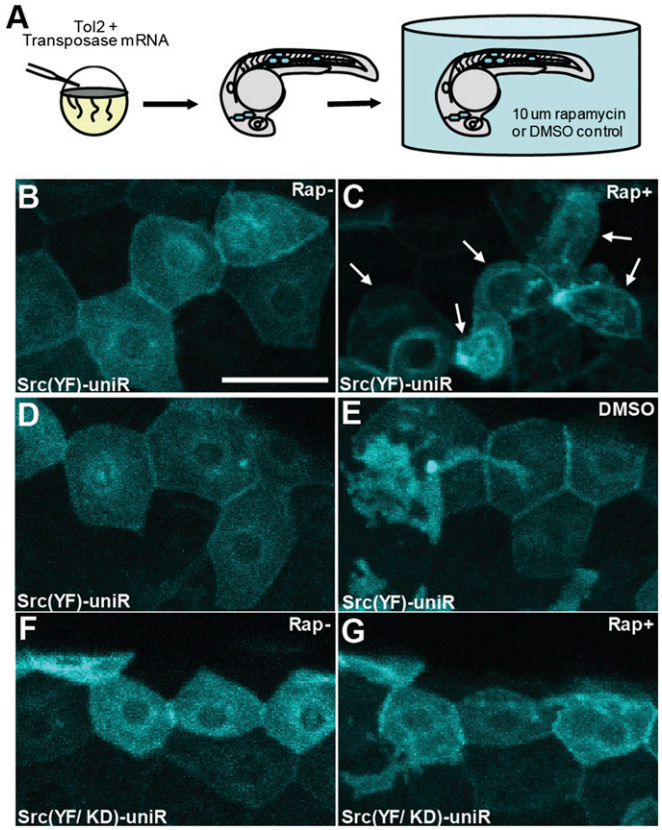

Fig. 4. Activation of Src induces cell changes in zebrafish epidermal cells. (*A*) Synthetic transposase mRNA was coinjected with the Tol2 Krt4 Src (YF)-uniRapR-cerulean plasmid into one-cell zebrafish embryos, resulting in mosaic expression of Src-uniRapR in the epidermis. Epidermal cells with characteristic flat honeycomb morphology were selected and imaged before (*B* and *F*) and after (*C* and *G*) 16 h of rapamycin treatment. (*C*) Epidermal cells expressing Src (YF)-uniRapR-cerulean in zebrafish embryos exposed to 10 μM rapamycin become rounded and undergo dynamic cell shape changes. White arrows indicate an epidermal cell before and after each treatment. Control epidermal cells expressing Src (YF)-uniRapR-cerulean in vehicle (i.e., DMSO) (*D* and *E*) or expressing the kinase-dead construct Src (YF/KD)-uniRapR-cerulean in rapamycin (*G*) have a static morphology and do not undergo dynamic cell shape changes. (Scale bar: 30 μm.)

Discussion

Design of a broadly applicable artificial regulatory domain has been challenging for the following reasons: (*i*) the protein should be able to adopt multiple states that can be "switched" by exogenous stimulation, i.e., ligand binding; (*ii*) the designed switch should be transferable, i.e., its action must be predictable and reproducible in a variety of host proteins; and (*iii*) the protein must be readily insertable into the host protein without significantly destabilizing it. We have solved these problems by designing a single-chain protein that can be regulated by a small molecule. Control of activity via small-molecule binding can be achieved by harnessing protein–protein interactions that occur in the presence of ligands, for example type 2C protein phosphatase ABI1/abscisic acid/PYR1-like (PYL1) (29) or FKBP12/rapamycin/FRB (20). Here we use the FKBP12/rapamycin/FRB complex because a photoactivable version of rapamycin is available, potentially making uniRapR a tool for spatial as well as temporal control of protein activity (30). Also, nonimmunosuppressive rapamycin analogues (31), such as C-16-(S)-3-methylindolerapamycin (iRap), can be used for minimal perturbation of normal physiology in animal studies. The *iRap* was proven to be innocuous in living cells (32). Here we show that Src-uniRapR is also active in the presence of *iRap* (Fig. S7). uniRapR can potentially be applied to a wide range of rapidly activating, allosteric signaling proteins. The dynamic behavior of a particular protein in a signaling pathway can be investigated by using a uniRapR protein analogue to activate the proteins with a resolution of minutes. Moreover, by inserting uniRapR into putative allosteric loops in a protein of interest, allosteric sites that are coupled can be experimentally identified.

We selected Src kinase as a proof-of-concept system to be tested in HeLa cells and zebrafish tissue because the specific role of this Src family member in cell motility is unclear. The roles of individual Src family members have proven to be difficult to dissect by using traditional approaches because of the functional redundancy and structural similarity of the Src family kinases (SFKs). SFKs are involved in many cellular processes, including transcription, differentiation, proliferation, development, motility, and cell death, and the majority of them have been identified as cellular oncogenes (27, 33). By using a uniRapR version of SFK members including Yes, Fyn, Lyn, Lck, Hck, Blk, Fgr, and Yrk kinases, differential roles of these proteins in cell motility can ultimately be elucidated.

An important advantage of uniRapR is its practical use in animals. Light-dependent control can be useful at the single-cell level, but uniRapR can provide activity control with the small molecule rapamycin even within deep tissues, where light cannot penetrate. To investigate the effect of Src kinase activation on a higher-order process such as intercellular communication in animals, a significant process involved in tissue development, repair, immune response, and homeostasis (27, 33), we tested uniRapR Src in living zebrafish epidermal tissue. We demonstrated that activation of Src kinase leads to a decrease in communication between cells, consistent with its oncogenic role in metastasis. The dynamic behavior of proteins downstream of Src, such as connexin 43 or Cas, that are involved in intercellular communication (34), will be the subject of future study.

UniRapR is a unique example of an insertable, transferable, and ligand-controllable protein switch. This switch has widespread potential applications for understanding signaling pathways involving kinases, a glimpse of which is offered by the unique phenotypes we demonstrate in mammalian cells and zebrafish tissue upon Src kinase activation. The potentially wide applicability of uniRapR is underscored by the structural conservation of kinases and the allosteric properties of many signaling proteins.

Materials and Methods

Detailed experimental and computational procedures are presented in *SI Materials and Methods*. In short: (*i*) DNA construction of the uniRapR domain and kinase-uniRapR constructs with all mutants was performed by using QuikChange PCR (Table S1). (*ii*) Computational design, modeling, and computational analysis of uniRapR and Src-uniRapR structures were performed by using replica-exchange and equilibrium DMD simulations (35) and Medusa modeling kit (36, 37) (Fig. S1 and Table S2). To analyze replica-exchange DMD simulations, the weighted histogram analysis method (WHAM) (38) was used to estimate thermodynamic properties of the uniRapR domain. (*iii*) Immunoprecipitation and in vitro kinase assays were as performed previously described (14). HEK293T cells expressing constructs were lysed, and protein constructs were pulled down and tested with the paxillin and poly-Glu-Tyr (E4Y) as Src and FAK substrate, and ATF2 as p38 substrate. The binding of the proteins to antibody-conjugated beads and phosphorylation of substrates were confirmed with Western Blotting. The enzymatic activities of immunoprecipitated constructs were determined by measuring the transfer rate of γ-^{32}P from radioactive ATP to substrate peptide E4Y. (*iv*) Live cell imaging was performed by using HeLa cells with an Olympus IX-81 microscope equipped with a ZDC focus drift compensator and a Photometrics CoolSnap ES2 CCD camera (Roper Photometrics). (*v*) Imaging of live zebrafish embryo epidermis tissue was performed with a confocal microscope (FluoView FV1000; Olympus).

ACKNOWLEDGMENTS. We thank Srinivas Ramachandran, Elizabeth Proctor, and Rachel Redler for critical comments on the manuscript. O.D. is a Howard Hughes Medical Institute International Student Research Fellow. This work

was supported by National Institutes of Health Awards R01GM080742 (to N.V.D.), U01GM094663 (to K.M.H.), and R01GM102924 (to K.M.H.); National Institute of Environmental Health Sciences Award ES007015 (to C.M.F.); and National Cancer Institute Award CA157322 (to C.M.F.).

1. Regan L, DeGrado WF (1988) Characterization of a helical protein designed from first principles. *Science* 241(4868):976–978.
2. Dahiyat BI, Mayo SL (1997) De novo protein design: Fully automated sequence selection. *Science* 278(5335):82–87.
3. Kuhlman B, et al. (2003) Design of a novel globular protein fold with atomic-level accuracy. *Science* 302(5649):1364–1368.
4. Allen BD, Mayo SL (2010) An efficient algorithm for multistate protein design based on FASTER. *J Comput Chem* 31(5):904–916.
5. Ambroggio XI, Kuhlman B (2006) Design of protein conformational switches. *Curr Opin Struct Biol* 16(4):525–530.
6. Yanover C, Fromer M, Shifman JM (2007) Dead-end elimination for multistate protein design. *J Comput Chem* 28(13):2122–2129.
7. Havranek JJ, Harbury PB (2003) Automated design of specificity in molecular recognition. *Nat Struct Biol* 10(1):45–52.
8. Korendovych IV, et al. (2011) Design of a switchable eliminase. *Proc Natl Acad Sci USA* 108(17):6823–6827.
9. Ostermeier M (2009) Designing switchable enzymes. *Curr Opin Struct Biol* 19(4): 442–448.
10. Kholodenko BN, Hancock JF, Kolch W (2010) Signalling ballet in space and time. *Nat Rev Mol Cell Biol* 11(6):414–426.
11. Dueber JE, Yeh BJ, Chak K, Lim WA (2003) Reprogramming control of an allosteric signaling switch through modular recombination. *Science* 301(5641):1904–1908.
12. Lee J, et al. (2008) Surface sites for engineering allosteric control in proteins. *Science* 322(5900):438–442.
13. Golynskiy MV, Koay MS, Vinkenborg JL, Merkx M (2011) Engineering protein switches: Sensors, regulators, and spare parts for biology and biotechnology. *ChemBioChem* 12(3): 353–361.
14. Karginov AV, Ding F, Kota P, Dokholyan NV, Hahn KM (2010) Engineered allosteric activation of kinases in living cells. *Nat Biotechnol* 28(7):743–747.
15. Wu YI, et al. (2009) A genetically encoded photoactivatable Rac controls the motility of living cells. *Nature* 461(7260):104–108.
16. Huala E, et al. (1997) Arabidopsis NPH1: A protein kinase with a putative redox-sensing domain. *Science* 278(5346):2120–2123.
17. Harper SM, Neil LC, Gardner KH (2003) Structural basis of a phototropin light switch. *Science* 301(5639):1541–1544.
18. Schreier B, Stumpp C, Wiesner S, Höcker B (2009) Computational design of ligand binding is not a solved problem. *Proc Natl Acad Sci USA* 106(44):18491–18496.
19. Banaszynski LA, Liu CW, Wandless TJ (2005) Characterization of the FKBP·rapamycin·FRB ternary complex. *J Am Chem Soc* 127(13):4715–4721, and erratum (2006) 128(49):15928.
20. Choi J, Chen J, Schreiber SL, Clardy J (1996) Structure of the FKBP12-rapamycin complex interacting with the binding domain of human FRAP. *Science* 273(5272):239–242.
21. Grishin NV (2001) Fold change in evolution of protein structures. *J Struct Biol* 134(2-3): 167–185.
22. Ding F, Tsao D, Nie H, Dokholyan NV (2008) Ab initio folding of proteins with all-atom discrete molecular dynamics. *Structure* 16(7):1010–1018.
23. Dagliyan O, Proctor EA, D'Auria KM, Ding F, Dokholyan NV (2011) Structural and dynamic determinants of protein-peptide recognition. *Structure* 19(12):1837–1845.
24. Suel GM, Lockless SW, Wall MA, Ranganathan R (2003) Evolutionarily conserved networks of residues mediate allosteric communication in proteins. *Nat Struct Biol* 10(1):59–69.
25. Sharma S, Ding F, Dokholyan NV (2007) Multiscale modeling of nucleosome dynamics. *Biophys J* 92(5):1457–1470.
26. Kidd BA, Baker D, Thomas WE (2009) Computation of conformational coupling in allosteric proteins. *PLOS Comput Biol* 5(8):e1000484.
27. Parsons SJ, Parsons JT (2004) Src family kinases, key regulators of signal transduction. *Oncogene* 23(48):7906–7909.
28. Lietha D, et al. (2007) Structural basis for the autoinhibition of focal adhesion kinase. *Cell* 129(6):1177–1187.
29. Melcher K, et al. (2010) Identification and mechanism of ABA receptor antagonism. *Nat Struct Mol Biol* 17(9):1102–1108.
30. Karginov AV, et al. (2011) Light regulation of protein dimerization and kinase activity in living cells using photocaged rapamycin and engineered FKBP. *J Am Chem Soc* 133(3):420–423.
31. Dickman DA, et al. (2000) Antifungal rapamycin analogues with reduced immunosuppressive activity. *Bioorg Med Chem Lett* 10(13):1405–1408.
32. Inoue T, Heo WD, Grimley JS, Wandless TJ, Meyer T (2005) An inducible translocation strategy to rapidly activate and inhibit small GTPase signaling pathways. *Nat Methods* 2(6):415–418.
33. Thomas SM, Brugge JS (1997) Cellular functions regulated by Src family kinases. *Annu Rev Cell Dev Biol* 13:513–609.
34. Shen YQ, et al. (2007) SRC utilizes Cas to block gap junctional communication mediated by connexin43. *J Biol Chem* 282(26):18914–18921.
35. Dokholyan NV, Buldyrev SV, Stanley HE, Shakhnovich EI (1998) Discrete molecular dynamics studies of the folding of a protein-like model. *Fold Des* 3(6):577–587.
36. Yin SY, Ding F, Dokholyan NV (2007) Eris: An automated estimator of protein stability. *Nat Methods* 4(6):466–467.
37. Ding F, Yin SY, Dokholyan NV (2010) Rapid flexible docking using a stochastic rotamer library of ligands. *J Chem Inf Model* 50(9):1623–1632.
38. Kumar S, Bouzida D, Swendsen RH, Kollman PA, Rosenberg JM (1992) The weighted histogram analysis method for free-energy calculations on biomolecules. 1. The method. *J Comput Chem* 13(8):1011–1021.

Supporting Information

Dagliyan et al. 10.1073/pnas.1218319110

SI Materials and Methods

DNA Construction. All restriction enzymes were purchased from New England Biolabs. All site-directed mutagenesis and gene insertion experiments were performed with the QuikChange mutagenesis kit (Stratagene). PCR products were used as megaprimers for QuikChange mutagenesis reactions (Table S1). The uniRapR domain was created by using PCR such that the 5′- and 3′-end sequences anneal at the desired insertion site within the Src, focal adhesion kinase (FAK), and p38 constructs.

Modeling of uniRapR and Src-uniRapR Structures. To model uniRapR, we removed the first 20 residues from FKBP12 [Protein Data Bank (PDB) ID code 1FAP] by using PyMol (www.pymol.org), so that the two termini are close in space for insertion. We built a circularly permuted FRB by excising at Asn2093 and joining the N- and C-termini together. We removed first four unstructured residues of FRB and connected the two termini with a peptide linker (PPGPGSG). To build a single-chain protein, we excised FKBP12 in Pro88 and connected FRB-G2092 to FKBP12-Gly89 and FKBP12-His87 to FRB-Val2094 with corresponding linkers (Fig. S2). We optimized the complex structure by minimizing the energy by using all-atom discrete molecular dynamics (DMD) simulations. We kept the unmodified regions of FKBP12 and FRB molecules static, whereas linkers were allowed to move to sample conformation and form peptide bonds under the peptide bond constraints between FKBP12/FRB and linkers.

Similarly, we modeled Src-uniRapR by excising the catalytic domain of Src at peptide bond of N287-G288 (PDB ID code 1Y57) and joining the termini of Src insertion loop and uniRapR with corresponding linkers, GPG. We used the model structures after energy minimization to perform replica-exchange simulations to characterize the folding thermodynamics or constant temperature simulations to probe the conformational dynamics. To model the rapamycin-bound state, we applied constraints (Table S2) between rapamycin and subdomain-A similar to interactions of rapamycin with FKBP12 in the crystal structure.

Computational Analysis of uniRapR. We performed all-atom DMD simulations to study the conformational dynamics of uniRapR. A complete description of the DMD algorithm can be found elsewhere (1, 2). We performed replica-exchange DMD simulations to estimate the folding thermodynamics. We used 18 replicas with temperatures ranging from 0.52 kcal/mol·k_B (~260 K) to 0.75 kcal/mol·k_B (~390 K), with an increment of 0.02 kcal/mol·k_B (0.01 kcal/mol·k_B between 0.64 kcal/mol·k_B and 0.72 kcal/mol·k_B). The length of each simulation is 1×10^6 time units (~50 ns). We applied the weighted histogram analysis method to estimate thermodynamic properties of the uniRapR domain. Next, we computed the partition function, $Z = \int \rho(E) exp(-E/k_B T) dE$, which allowed us to derive the specific heat at different temperatures. We also calculated rmsd and tail distance of subdomain-A as function of temperature by using weighted histogram analysis.

We performed a constant temperature simulation of Src-uniRapR at 0.5 kcal/mol·k_B. This is below the folding transition temperature of uniRapR; therefore, the inserted domain stays folded whereas the DMD simulation optimizes its relative orientation with respect to Src. We computed distances between centers of masses of uniRapR subdomains for multiple trajectories. Similar to subdomain-A insertion into subdomain-B, we applied peptide bond constraints to insert uniRapR into Src kinase and performed equilibrium DMD simulations. We computed normalized dynamic correlation matrices (4) to determine the Src activation mechanism. To exclude protein drift when computing residues' fluctuations correlations and root mean square fluctuations, we translated the center of mass of the protein to the origin and aligned each snapshot with respect to the average structure.

Immunoprecipitation and in Vitro Kinase Assay. Anti-myc and anti-FLAG antibodies were purchased from Millipore and Sigma, respectively. Anti–phospho-paxillin-pTyr31 and anti-GFP (JL8) antibodies were purchased from Biosource and Clontech, respectively. Anti–phospho-ATF2 was purchased from Santa Cruz. Rapamycin was purchased from Sigma. Radioactive ATP was purchased from MP Biomedical (7,000 Ci/mmol). Poly-Glu-Tyr (4:1) peptide (E4Y) was purchased from Sigma. HEK293T cells were transfected with 2 μg of DNA constructs by using Fugene6 reagent (Roche). Cells were treated with rapamycin or an equivalent volume of ethanol (solvent of rapamycin solution). Cells expressing Src or FAK constructs were then washed with cold PBS solution and lysed with 20 mM Hepes-KOH, pH 7.8, 50 mM KCl, 100 mM NaCl, 1 mM EGTA, 1% Nonidet P-40, 1 mM NaF, 0.1 mM Na_3VO_4, and Roche protease inhibitor mixture. Cells expressing p38 were lysed with 20 mM Tris, pH 7.5, 150 mM NaCl, 1 mM EGTA, 1 mM EDTA, 1% Triton X-100, 0.5% Nonidet P-40, 20 mM NaF, 0.2 mM Na_3VO_4, and Roche protease inhibitor mixture. Cells treated with rapamycin were lysed with the appropriate lysis buffer containing the corresponding rapamycin concentration. Cleared lysates were incubated with protein G beads attached to anti-myc (for Src and FAK) or anti-FLAG (for p38) antibody for 2 h. The beads were washed three times with wash buffer (20 mM Hepes-KOH, pH 7.8, 50 mM KCl, 100 mM NaCl, 1 mM EGTA, 1% Nonidet P-40) and then with kinase buffer (25 mM Hepes-KOH, pH 7.5, 5 mM $MgCl_2$, 0.5 mM EGTA, 0.005% BRIJ-35) for Src and FAK assays. For p38 assays, beads were washed with p38 lysis buffer and then with p38 kinase buffer (25 mM Hepes-KOH, pH 7.4, 10 mM $MgCl_2$, 25 mM β-glycerophosphate, 4 mM DTT, 0.1 mM Na_3VO_4). For Src and FAK assays, 20 μL of bead suspension were used in the presence of purified substrate paxillin (0.05 mg/mL) and cosubstrate ATP (0.1 mM). For p38 assays, 1 μg purified ATF2 and ATP (0.5 mM) in 40 μL of kinase buffer were mixed with bead suspension for the reaction.

To obtain reaction kinetics, we measured the activity of Src-uniRapR at different time points to determine initial velocities with varying peptide (E4Y) and ATP concentrations (5). We performed the assay as described in the protocol for the Src Kinase Assay Kit (Upstate Biotechnology). At each rapamycin concentration, we titrated the peptide substrate at fixed ATP concentrations. The reaction temperature was at 30 °C. The reaction was stopped with 0.75% phosphoric acid. The phosphorylated substrate was separated from residual [γ-^{32}P]ATP using P81 phosphocellulase paper. The bound radioactivity was quantified with a 1214 RackBeta scintillation counter (LKB).

Live Cell Imaging. HeLa cells were plated on fibronectin-coated coverslips (10 mg/mL fibronectin for 1 h at 37 °C; Sigma) and incubated for 3 h. in DMEM supplemented with 10% (vol/vol) FBS. Then DMEM was replaced with L-15 imaging medium (Invitrogen) supplemented with 5% (vol/vol) FBS. An open heated chamber (Warner Instruments) was used to maintain the cells. Live cell imaging was performed with an Olympus IX-81 microscope equipped with a ZDC focus drift compensator. Images were collected by using a Photometrics CoolSnap ES2 CCD

camera (Roper Photometrics). Metamorph software (Molecular Devices) was used to control the microscope and to acquire and process images at each time point. To calculate cell area, each cell was manually traced around its edge, and a binary mask was created by using Metamorph. Values were normalized to be 1 at the time point before addition of rapamycin.

Imaging of Live Zebrafish. Approximately 5 nL of a DNA–RNA solution containing 20 ng/μL circular DNA of a transposon-donor plasmid and 40 ng/μL transposase mRNA were injected into one-cell zebrafish embryos. Twenty-four hours after the injection, individual embryos with epidermal expression of Src were imaged before and after 16 h of exposure to 10 μM rapamycin (Invitrogen) or vehicle (DMSO). Only epidermal cells with characteristic flat honeycomb morphology were selected for analysis because robust transgene expression induces cell defects before treatment. Imaging was performed on a confocal microscope (FluoView FV1000; Olympus).

1. Dokholyan NV, Buldyrev SV, Stanley HE, Shakhnovich EI (1998) Discrete molecular dynamics studies of the folding of a protein-like model. *Fold Des* 3(6):577–587.
2. Ding F, Tsao D, Nie H, Dokholyan NV (2008) Ab initio folding of proteins with all-atom discrete molecular dynamics. *Structure* 16(7):1010–1018.
3. Kumar S, Bouzida D, Swendsen RH, Kollman PA, Rosenberg JM (1992) The weighted histogram analysis method for free-energy calculations on biomolecules. 1. The method. *J Comput Chem* 13(8):1011–1021.
4. Sharma S, Ding F, Dokholyan NV (2007) Multiscale modeling of nucleosome dynamics. *Biophys J* 92(5):1457–1470.
5. Cole PA, Burn P, Takacs B, Walsh CT (1994) Evaluation of the catalytic mechanism of recombinant human Csk (C-terminal Src kinase) using nucleotide analogs and viscosity effects. *J Biol Chem* 269(49):30880–30887.
6. Yin SY, Ding F, Dokholyan NV (2007) Eris: An automated estimator of protein stability. *Nat Methods* 4(6):466–467.
7. Ding F, Yin SY, Dokholyan NV (2010) Rapid flexible docking using a stochastic rotamer library of ligands. *J Chem Inf Model* 50(9):1623–1632.
8. Suel GM, Lockless SW, Wall MA, Ranganathan R (2003) Evolutionarily conserved networks of residues mediate allosteric communication in proteins. *Nat Struct Biol* 10(3):59–69.

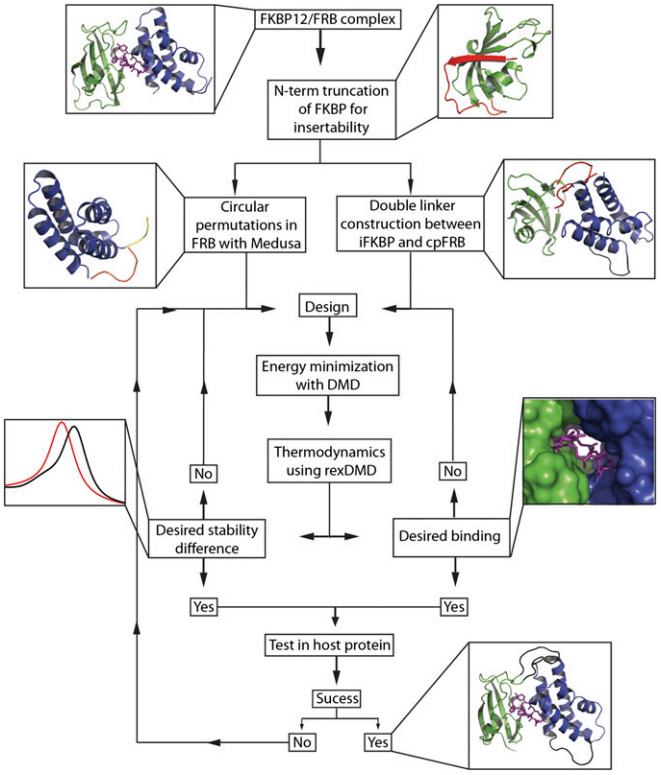

Fig. S1. Design protocol. Two proteins interact in the presence of ligand are chosen as a template structure, such as FKBP (green)/rapamycin (magenta)/FRB (blue) complex (PDB ID code 1FAP). To obtain an insertable design, termini should be close to each other. In this study, for minimal perturbation, we selected a β-sheet hairpin at the C terminal of FKBP12 by removing the first 20 residues. To make a chimeric protein making a hinge motion with a double linker, several designs that include circular permutations of FRB and FKBP linked with different lengths of linkers are considered. These designs are built by using Medusa (6, 7) and DMD by first keeping the domains fixed and allowing the linkers flexible. After energy minimization with all-atom DMD simulations, replica exchange DMD simulations are performed to obtain thermodynamic properties of the designs. If there is a difference in stability in the presence of ligand compared with absence of the ligand, the design is kept. Also, if two subdomains of the design bind to each other only in the presence of ligand, the design is kept. In the case of success, next step is to test switch behavior in a host protein. The insertion site for the designed switch can be determined with our cross-correlation analysis (4) or any other method (8) that provides allosterically coupled sites. A distant site that is allosterically coupled to catalytic site or cosubstrate binding site, i.e., ATP binding site, can be selected for the switch insertion. If the control of host activity that is caged with the designed switch is not robust, a different length of double linker can be used. For example, in the p38 case, the control is more robust if uniRapR is inserted without the default GPG linker.

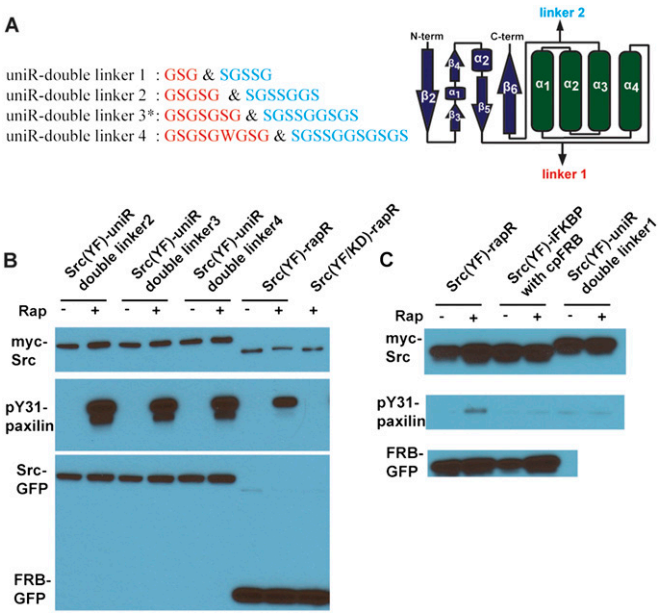

Fig. S2. Testing different lengths of double linkers between uniRapR subdomains. (*A*) Double linker connecting the subdomains-A and -B are shown in red and cyan. The linker with asterisks is the one used in the current version of uniRapR. (*B*) Src-uniRapR-cerulean-myc constructs were expressed in HEK293T cells. Cell lysates were blotted with anti-GFP to confirm the expression of the construct. In dimerization-based switch (rapR), coexpressed FRB was also tested with anti-GFP. Cell lysates were pulled down with anti-myc and mixed with substrate paxillin in the presence of ATP for 10 min. Reaction suspension was blotted with anti-myc to confirm the binding, with anti–pY31-paxilin to confirm the phosphorylation of the substrate. Linker 2 is the one required for functional uniRapR. (*C*) The design with truncated linker 2 (linker 1) does not provide control over Src.

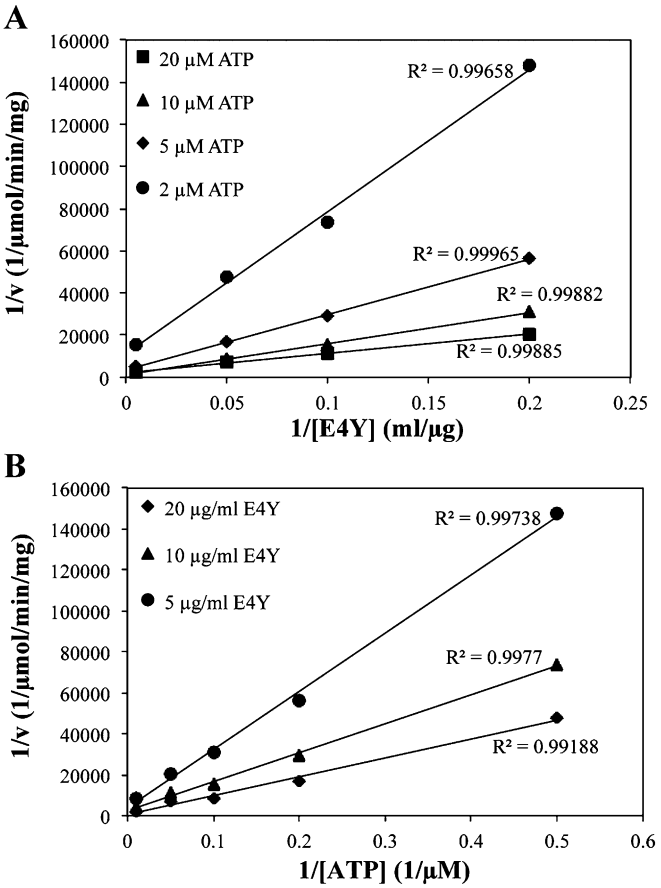

Fig. S3. Substrate kinetics analysis of Src-uniRapR. (*A*) Plot of 1/velocity versus 1/[E4Y] at four fixed ATP concentrations. (*B*) Plot of 1/velocity versus 1/[ATP] at three fixed E4Y concentrations.

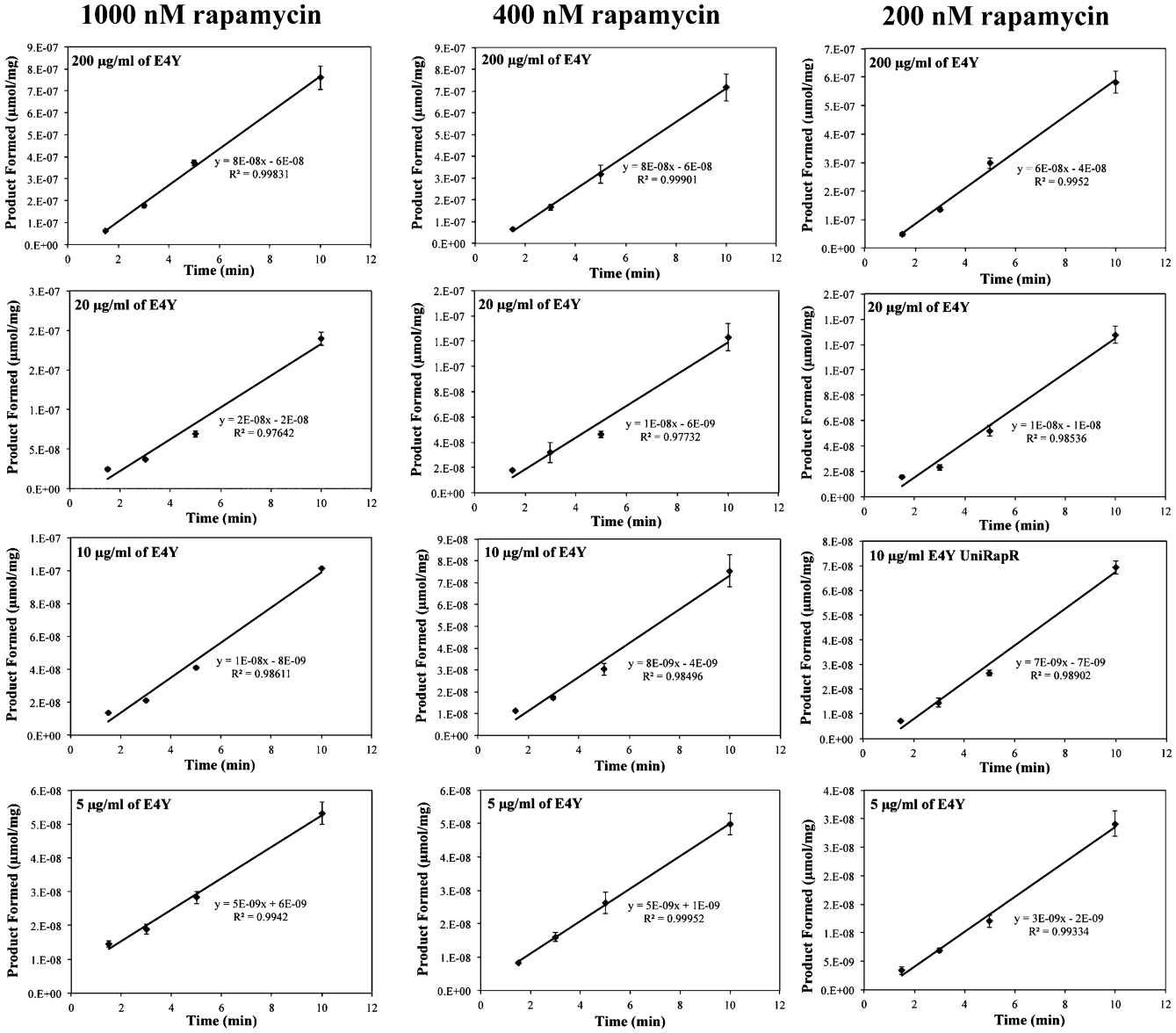

Fig. S4. Velocity of Src-uniRapR at various peptide concentrations (5–200 µg/mL) and rapamycin concentrations (200–1,000 nM).

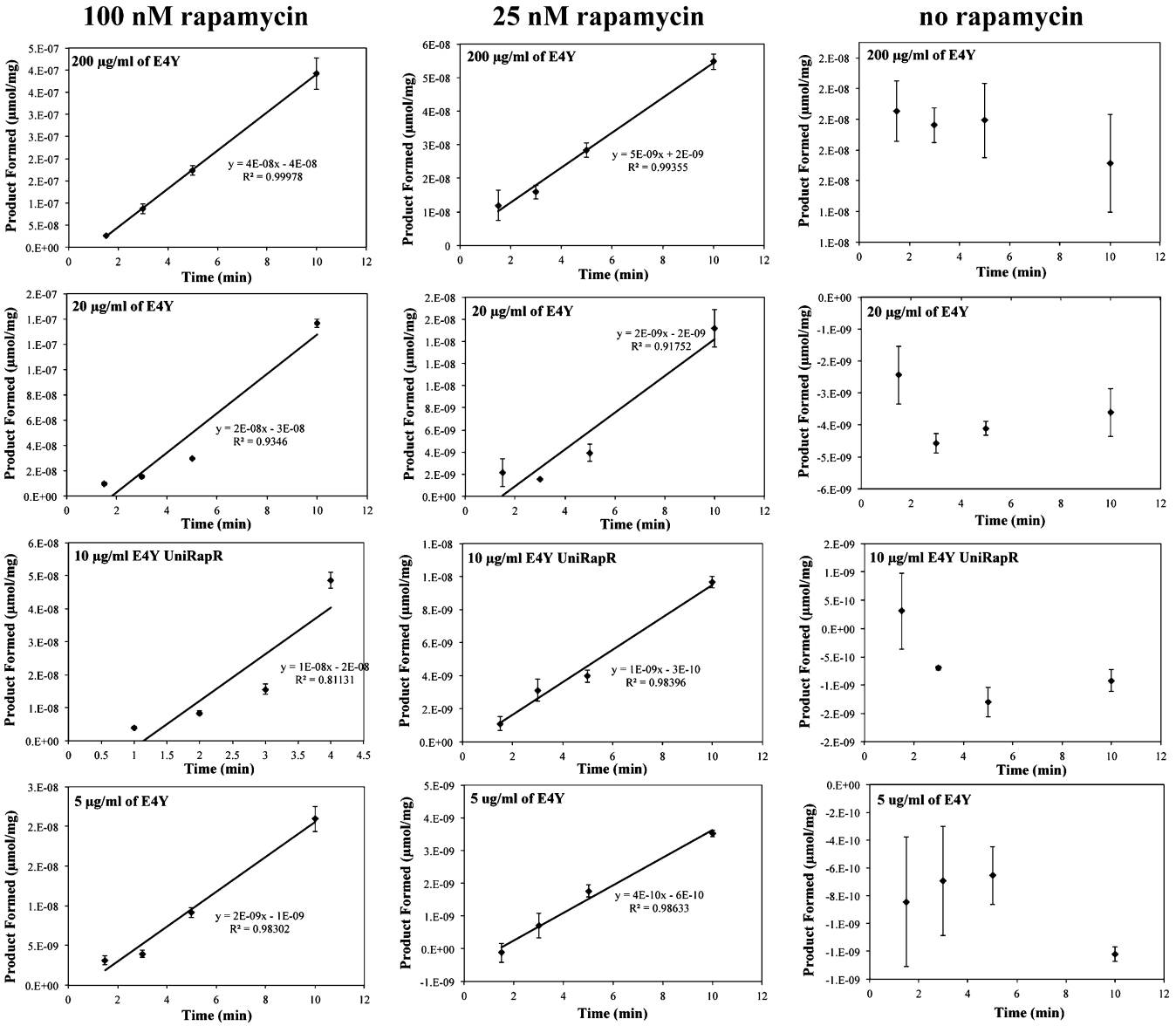

Fig. S5. Velocity of Src-uniRapR at various peptide concentrations (5–200 µg/mL) and rapamycin concentrations (0–100 nM).

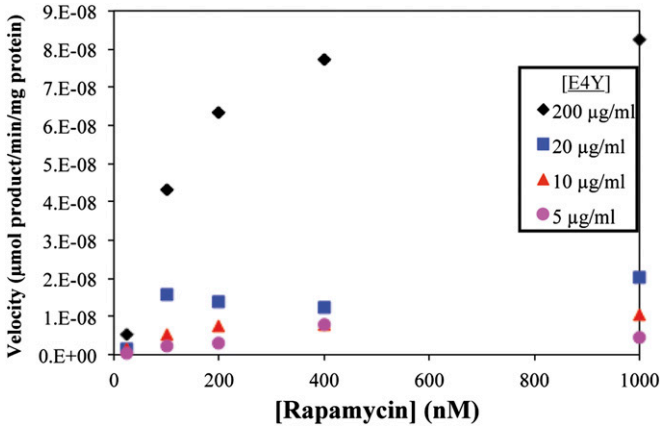

Fig. S6. Rapamycin-dependent velocity profile of Src-uniRapR.

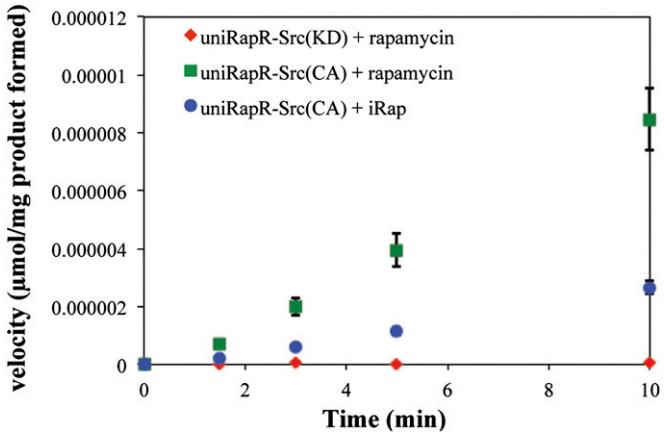

Fig. S7. The velocity of Src (CA)-uniRapR, Src(KD)-uniRapR in the presence of rapamycin, and nonimmunosuppressive rapamycin analogue *iRap*.

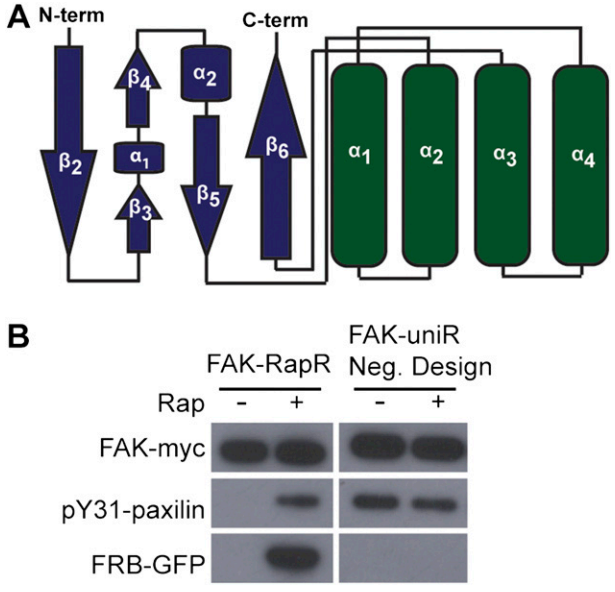

Fig. S8. A different design with different connections between secondary structure components (*A*) does not provide any control over FAK (*B*).

Table S1. Primers used for PCR

Description	Primer sequence (5′ to 3′ forward and 5′ to 3′ reverse)
To replace α4 helix with SSG in FRB	gtgcaggaagtacatgaaatcagggtcatcagggtaaccgtacgacgtaccagactacg
	cgtagtctggtacgtcgtacggttaccctgatgaccctgatttcatgtacttcctgcac
To get megaprimer for cpFRB	Ctcagatctcgagctcaagcttcgaattcagtcaaggacctcctccaagcctggg
	caggccttcatgccacatctcatgccagagacctgatccaggtcctggaggacctgagattcgtcggaacacatgataatagag
To get megaprimer for Src-uniRapR-double-linker1	Ccagattatgcctatggtgccactgggcacggatcaggcgtcaaggacctcctccaagcc
	gacgagagtggcatgtggtgggatgatgccccctgatgaccctgatttcatgtac
To convert double-linker1 to double-linker2	gattatgcctatggtgccactgggcacggttcgggatcaggcgtcaaggacctcctc
	gacgagagtggcatgtggtgggatgattccggagcccccctgatgaccctgatttcatg
To convert double-linker1 to double-linker3	gattatgcctatggtgccactgggcacggttcgggctccggatcaggcgtcaaggacctcctc
	gacgagagtggcatgtggtgggatgatgcctgatccggagcccccctgatgaccctgatttcatg
To convert double-linker1 to double-linker4	gattatgcctatggtgccactgggcacggttcgggctccgggtggggatcaggcgtcaaggacctcctc
	gacgagagtggcatgtggtgggatgatccccgagcctgatccggagcccccctgatgaccctgatttcatg
To convert linker1 to polyProline linker of double-linker3	gattatgcctatggtgccactgggccccctccgccacccccacctccggtcaaggacctcctccaagcctg
	caggcttggaggaggtccttgaccggaggtgggggtggcggaggggggcccagtggcaccataggcataatc
To convert linker2 to poly-proline linker of double-linker3	gagtggtgcaggaagtacatgaaaccaccgccacctccgccacctccaccgccaatcatcccaccacatgccactctcg
	cgagagtggcatgtggtgggatgattggcggtggaggtggcggaggtggcggtggtttcatgtacttcctgcaccactc
Y271A (Y82A in original FKBP12 sequence)	gactatatctccagattatgccgctggtgccactgggcacggttcg
	cgaaccgtgcccagtggcaccagcggcataatctggagatatagtc
Src kinase dead mutation (D388R)	cggatgaactatgtgcaccggcgccttcgagccgccaatatcc
	ggatattggcggctcgaaggcgccggtgcacatagttcatccg
To insert uniRapR into FAK (F442-8 GPG)	cagtttggagatgtacatcaaggcgtgtacggcccaggaacctgcgtggtgcactacacc
	gtttttacatgttttgattgcaacagccaaacctgggccttccagttttagaagctccac
FAK kinase dead mutation (K454R)	ccagctttggctgttgcaatcagaacatgtaaaaactgtacttcgg
	ccgaagtacagtttttacatgttctgattgcaacagccaaagctgg
To insert uniRapR into P38 (PE)	gcctatggctcggtgtgtgctgcttttgatacatacctgagcccaggcacctgc
	cgacagcttcttaactgccacacgatgccccgtcaaagctggattgccttccag

Table S2. Atom pair constraints between C_β atom subdomain B and rapamycin

Subdomain B residue	Corresponding FRB residue in 1FAP	Rapamycin atom index	dmin, Å	dmax, Å
K76	K2095	C14	9.09	11.11
T79	T2098	C14	5.22	6.38
T79	T2098	C16	5.13	6.27
T79	T2098	C10	6.66	8.14
W82	W2101	C16	4.50	5.50
W82	W2101	C18	4.14	5.06
W82	W2101	C20	4.50	5.50
D83	D2102	C16	5.76	7.04
D83	D2102	C18	6.12	7.48
Y86	Y2105	C18	4.14	5.06
Y86	Y2105	C20	3.51	4.29
Y86	Y2105	C23	4.95	6.05
F89	F2108	C21	5.13	6.27
F89	F2108	C23	4.14	5.06
F89	F2108	C25	6.03	7.37
L111	L2031	C23	4.86	5.94
L111	L2031	C25	6.93	8.47
L111	L2031	C21	6.03	7.37
E112	E2032	C22	5.94	7.26
E112	E2032	C24	4.50	5.50
E112	E2032	C26	5.49	6.71
S115	S2035	C22	3.24	3.96
S115	S2035	C24	4.05	4.95
S115	S2035	C20	4.41	5.39
S115	S2035	C27	4.14	5.06
S115	S2035	C29	4.77	5.83
R116	R2036	C24	6.66	8.14
R116	R2036	C27	5.31	6.49
R116	R2036	C29	6.84	8.36
F119	F2039	C28	5.04	6.16
F119	F2039	C33	4.95	6.05
F119	F2039	C35	4.41	5.39
F119	F2039	C39	5.13	6.27
F119	F2039	C41	6.39	7.81

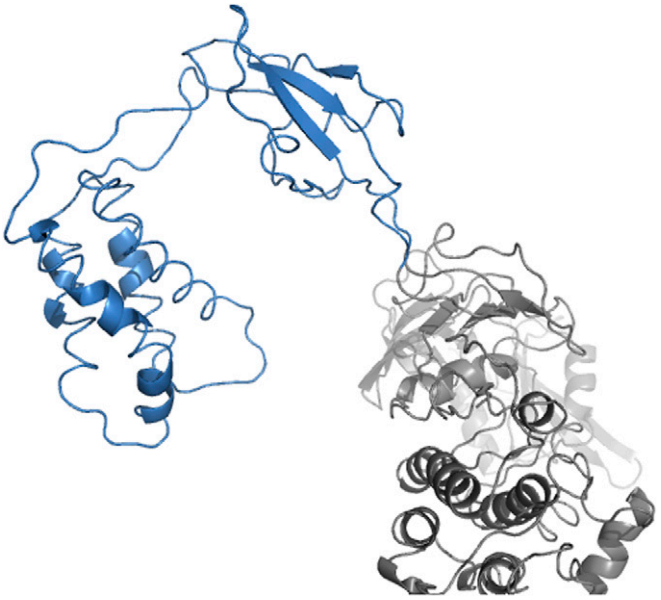

Movie S1. Subdomains of uniRapR do not bind to each other in the absence of rapamycin. Molecular dynamics simulation demonstrates free movement of the uniRapR (blue) inserted into the catalytic domain of Src kinase (gray). The simulations were performed as described in *Materials and Methods*.

Movie S1

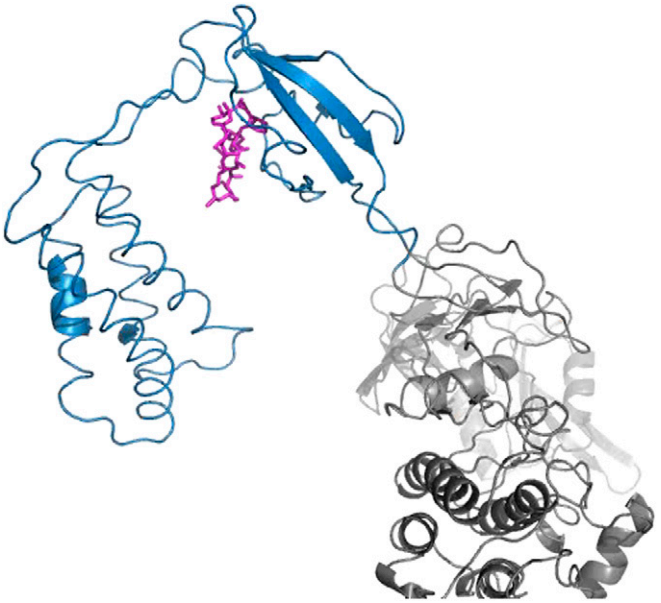

Movie S2. Subdomains of uniRapR do not bind to each other in the presence of rapamycin. Molecular dynamics simulation demonstrates binding of uniRapR subdomains (blue) inserted into the catalytic domain of Src kinase (gray) in the presence of rapamycin (magenta). The simulations were performed as described in *Materials and Methods*.

Movie S2

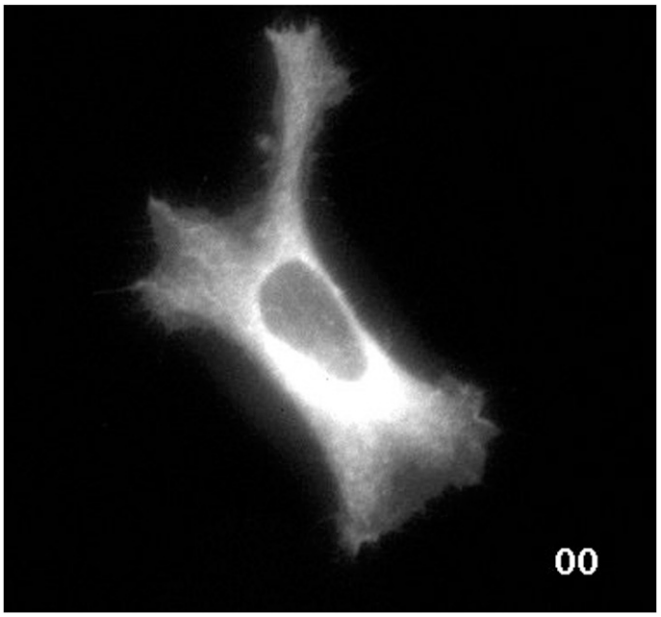

Movie S3. Spreading of HeLa cells upon temporal activation of Src with uniRapR shown with fluorescent imaging. HeLa cells transfected with mCerulean-uniRapR-Src (YF) were filmed for 30 min before and 60 min after addition of rapamycin. Fluorescent images were taken at 1-min intervals.

Movie S3

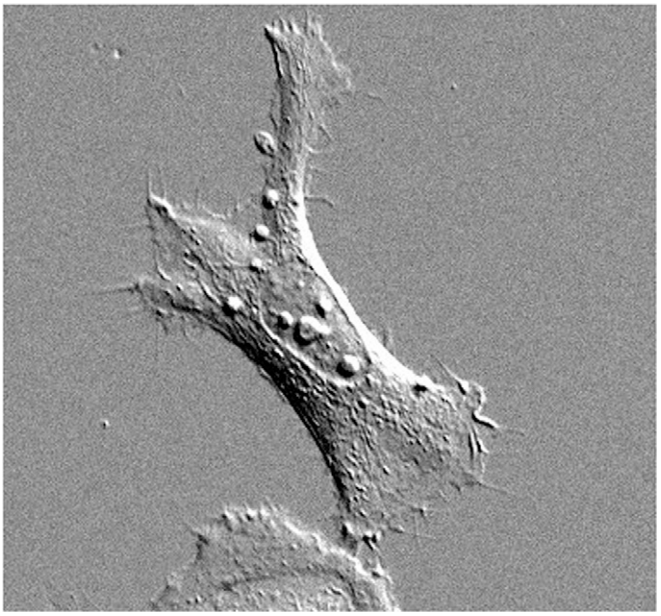

Movie S4. Spreading of HeLa cells upon temporal activation of Src with uniRapR shown with DIC imaging. HeLa cells transfected with mCerulean-uniRapR-Src (YF) and were filmed for 30 min before and 60 min after addition of rapamycin. DIC images were taken at 1-min intervals.

Movie S4